Reduced-scale study of the coupling between thermal and wind effects on the ventilation systems of nuclear facilities

T. Le Dez, J. Richard, C. Inard, N. Le Roux, F. Demouge, X. Faure, L. Ricciardi

International Journal of Ventilation, 2019 [DOI: 10.1080/14733315.2019.1693135]

Reduced-scale study of the coupling between thermal and wind effects on the ventilation systems of nuclear facilities

Thomas Le Dez, Jérôme Richard, Christian Inard, Nicolas Le Roux, François Demouge, Xavier Faure & Laurent Ricciardi

Abstract

To study heat and mass transfers inside nuclear facilities equipped with ventilation systems, a methodology was developed to carry out reduced-scale experiments for studying flows induced by thermal and wind effects simultaneously. The methodology was numerically validated on simple configurations and applied to a reference configuration representative of nuclear facilities. The effects of wind and thermal phenomena on heat and mass transfers in various ventilation situations (normal ventilation or ventilation switched off) and scenarios of heat supply were studied in wind tunnel experiments. The thermal sources that could be generated by an industrial process were reproduced experimentally with a helium injection. The objectives of this article are to present the scaling-down methodology and the main experimental results concerning the influence of thermal effects on airflows in the reduced-scale model. The effects of heat with or without wind on loss of building containment were also highlighted and analysed. Finally, the reliability of SYLVIA simulation software, which was used to support safety assessments in nuclear facilities, was analysed using the experimental results.

Keywords: Ventilation networks, similarity, non-isothermal flows, reduced-scale experiments, SYLVIA simulation software, nuclear facilities

1. Introduction

The nuclear industry is particularly concerned with the need to contain radioactive pollutants within power plants, laboratories or fuel treatment facilities. Thus, to support safety assessments in nuclear buildings, the SYLVIA simulation software called SYLVIA afterwards was developed by the Institut de Radioprotection et de Sûreté Nucléaire (IRSN) to predict airflow inside industrial ventilation systems in nominal, damage (ventilation shut down) or accident situations (e.g., a pressure tank fracture, fire or an overpressure scenario). Modelling airflow created by mechanical ventilation using SYLVIA has already been validated by experiments conducted on real facilities. Moreover, reduced-scale experiments have been conducted to study steady and transient isothermal flows inside complex buildings equipped with ventilation systems (Le Roux, Faure, Inard, Soares, & Ricciardi, 2012; 2013). Wind effects have also been taken into account in real facilities by acquiring experimental data on the mean pressure coefficients for buildings and chimneys with different geometries using wind tunnel tests, in order to validate a CFD code (ANSYS CFX) from these experimental results (Ricciardi, Gélain, & Soares, 2015). However, these studies only concerned isothermal flows.

Although in-depth studies have been conducted on a fire scenario in nuclear facilities (Prétrel, Le Saux, & Audouin, 2012; Vaux & Prétrel, 2013), coupling between wind and thermal effects may occur and thwart the mechanical ventilation effect. These combined effects have not yet been validated in SYLVIA. For this reason, experiments must be conducted to check the reliability of SYLVIA in terms of coupled wind and thermal effects. The most appropriate solution for experimentally studying wind and thermal effects in several airflow conditions is to conduct reduced-scale experiments in a wind tunnel. For this purpose, a similarity study of physical phenomena should first be performed to ensure that the reduced-scale and the full-scale flows are similar.

Although reduced-scale ventilation studies have been performed in buildings (Chen, Liu, & Chow, 2011; Hunt & Linden, 2001; 2005; Li et al., 2001), no appropriate methodology has been found to take into account wind effects and thermal flows inside complex buildings equipped with ventilation networks.

The present experimental approach is based on a reduced-scale helium protocol. Helium has already been used to reproduce and visualize a thermal flow through an opening (Lucchesi, Vauquelin, Pretrel, & Bournot, 2011) or inside a tunnel (Vauquelin & Megret, 2002). The use of helium simulates the large density differences to be studied. However, radiative transfer and heat loss to the walls are not taken into account (Vauquelin, 2008).

2. Methodology

2.1. Modelling of the ventilation system

The modelling of the ventilation system was based on the breakdown of the ventilation system into nodes and branches. Each node represents either a room or a junction between branches, where the mass balance is applied. Each branch represents either a passive component (duct, filter, leak), or a driving force (fans), where the integral kinetic energy theorem was applied.

In order to take into account the thermal effects, the energy balance equation must be also considered for each node. The formulation of the energy balance equation was based on the first law of thermodynamics. A detailed description of the equations used can be found in Le Roux (2011) and Le Dez (2016).

2.2. Similarity study

The development of the methodology consists in expressing the theoretical model in dimensionless form in order to reveal dimensionless parameters. Towards this end, the model was expressed in a dimensionless form by considering a reference value X_{ref} for each variable X. Then, a scaling-down methodology was applied for each variable between the full-scale and the reduced-scale of the ventilation system. The scale parameter is defined as the ratio of the reduced-scale and the full-scale reference value.

$$\bar{X} = \frac{X_{ref,reduced-scale}}{X_{ref,full-scale}} \quad (1)$$

Furthermore, the similarity study should take into account the restrictive conditions due to real configurations (room sizes, airflow rates) and experimental constraints (wind tunnel size, methodology used). Hence, by considering these conditions, the similarity is respected only by assuming three fixed scale parameters: the density scale, the flow rate scale, and the height scale. The conservation of the dimensionless numbers allowed to determine the remaining scale parameters. Details about the relations between fixed and calculated scale parameters given in Table 1 can be found in Le Dez (2016).

Table 1. Relations between fixed and calculated scale parameters.

Fixed scale parameters	Calculated scale parameters		
$\bar{\rho} = \Delta\rho$	$\bar{T} = \bar{\rho}$	$\bar{P} = \bar{U}^2$	$\bar{R}_{duct} = \frac{1}{\bar{S}^2} = \frac{\bar{h}}{\bar{Q}^2}$
$\bar{Q}$	$\bar{E}_s = \bar{\rho}\bar{Q}\bar{T}$	$\bar{m}_f = \bar{\rho}\bar{Q}$	$\bar{R}_{filter} = \frac{\bar{U}}{\bar{S}} = \frac{\bar{h}}{\bar{Q}}$
$\bar{h} = \bar{z}$	$\bar{U} = \sqrt{\bar{h}}$		$\bar{R}_{leak} = \frac{\bar{U}^{2-n}}{\bar{S}^n} = \frac{\bar{h}}{\bar{Q}^n}$

3. Experimental setup

3.1. Full-scale configuration

To study representative industrial facilities, a simplified configuration was designed which is shown schematically in Figure 1.

Figure 1. Schematic diagram of the simplified configuration.

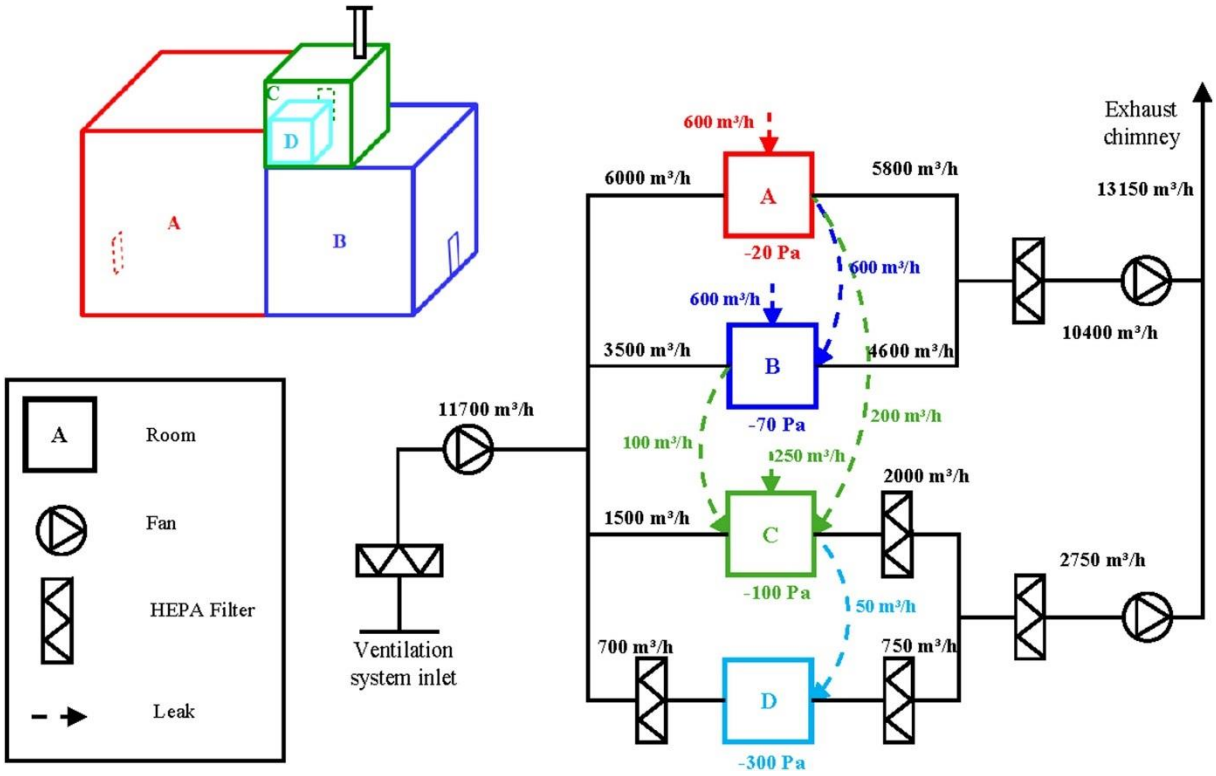

The configuration is composed of four rooms and represents a facility for which the highest-risk and thus the most confined rooms (i.e., rooms C and D) are placed near the top of the building. The thermal effects are maximised for these rooms. The configuration had three ventilation systems: a supply ventilation system for all four rooms, an exhaust ventilation system for rooms A and B, and an exhaust ventilation system for rooms C and D.

This configuration is not an actual one but a hypothetical case. Nevertheless, it has been designed in accordance with the ISO 17873 standard (ISO, 2014). The nuclear facilities containment must provide confinement of radioactive substances in the event of accidents. To this end, a dynamic containment which creates negative pressure in order to prevent any direct leakage from the confined rooms to the outside has to be implemented. For this purpose, the ISO 17873 standard provides the design and sizing rules in terms of pressures, number of HEPA filters and air change in accordance with the containment classes. So, this case study has the properties of a real case.

In addition, this case study is very useful for testing SYLVIA because it includes the main elements used for the dynamic containment of nuclear facilities, namely ventilation systems, rooms to be kept absolutely contained and leakage of the envelopes.

3.2. Set of scale parameters used

Table 2 gives the set of scale parameters of the reduced-scale model. For more details about the method used in order to fix and to calculate the values of the scale parameters, see Le Dez (2016).

Table 2. Set of scale parameters used to design the reduced-scale model.

Fixed scale parameters	Calculated scale parameters		
$\bar{\rho} = \Delta\rho = 1$	$\bar{T} = 1$	$\bar{\rho} = 1$	$\bar{R}_{duct} = \frac{1}{\bar{S}^2} = \frac{\bar{h}}{\bar{Q}^2} = 640$
$\bar{Q} = \frac{1}{80}$	$\bar{E}_s = \bar{\rho}\bar{Q}\bar{T} = \frac{1}{80}$	$\bar{P} = \bar{U}^2 = \frac{1}{10}$	$\bar{R}_{filter} = \frac{\bar{U}}{\bar{S}} = \frac{\bar{h}}{\bar{Q}} = 8$
$\bar{h} = \bar{z} = \frac{1}{10}$	$\bar{U} = \sqrt{\bar{h}} \approx \frac{1}{3}$	$\bar{m}_f = \bar{\rho}\bar{Q} = \frac{1}{80}$	$\bar{R}_{leak} = \frac{\bar{U}^{2-n}}{\bar{S}^n} = \frac{\bar{h}}{\bar{Q}^n} \approx 37\ (n = 1.35)$

3.3. Design of the reduced-scale models

A view and a schematic representation of the model, whose design was based on these characteristics, are presented in Figure 2.

Figure 2. View and plan of the reduced-scale model.

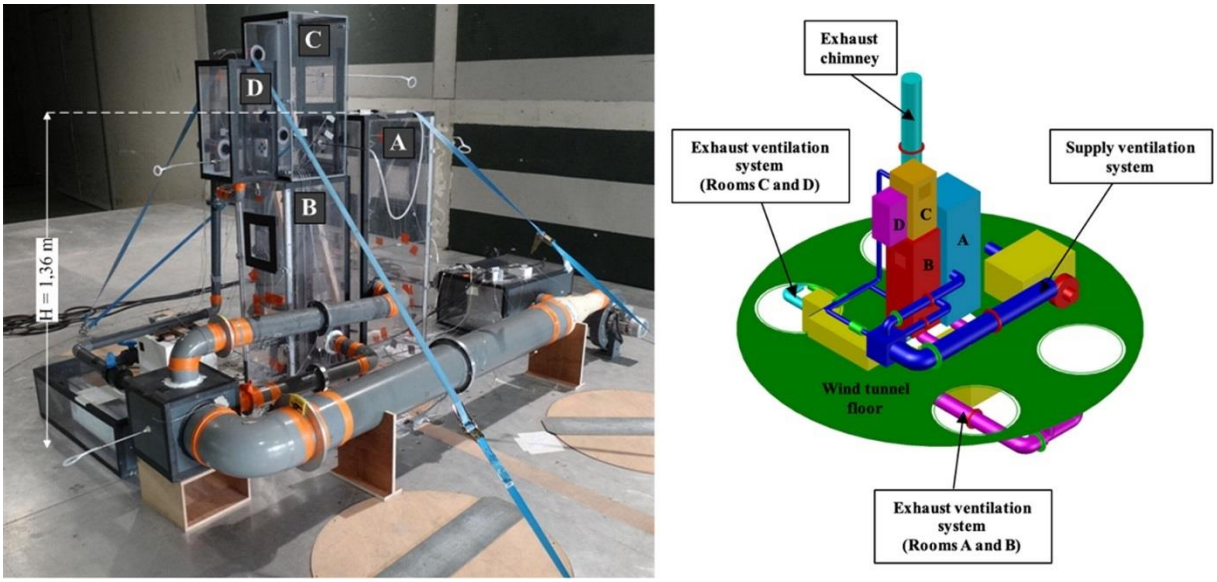

Each fan, equipped with a variable frequency controller, was chosen to satisfy the theoretical reduced-scale operating points presented in Table 3. These values were determined by applying the pressure scale *P* and the flow rate scale *Q* to the full-scale operating points.

Table 3. Reduced-scale operating points of the fans.

Fan	Reduced-scale operating points (Q - ΔP)
Supply fan	146.3 $m^3\ h^{-1}$–100 Pa
Exhaust fan of rooms A and B	130 $m^3\ h^{-1}$–115 Pa
Exhaust fan of rooms C and D	34.4 $m^3\ h^{-1}$–180 Pa

Internal leaks between the rooms and external leaks were included in order to simulate air flows through the building doors depending on their airtightness class. They were represented by calibrated perforated plates. These ones were dimensioned using the approach set out by Le Roux (Le Roux et al., 2012) for the choice of the thickness of the plate, the hole diameter and finally the number of holes for each plate. However, this approach did not take into account density variation. Thus, an experimental characterization of the law exponent was performed with a pure helium injection. Contrary to the isothermal case (Le Roux, 2011), the experimental apparatus was modified by replacing the fan with a helium injection system. The injection flow rate was controlled using a mass flow meter. In order to ensure that helium mixing was achieved, bends were added upstream of the plenum to decrease the well-mixing length. As an example, the power law equation of a plate with air and pure

helium is presented in Figure 3. The measured flow rate ("Q_m measured" on the figure) was obtained using an orifice plate for air and a mass flow meter for helium. It should be noted that the power law exponent is equal to 0.584 indicating a flow close to fully turbulent. A value near to one would have indicated a rather laminar flow.

Figure 3. Comparison between the measured flow rate and the flow rate obtained with the exponent law for air and pure helium.

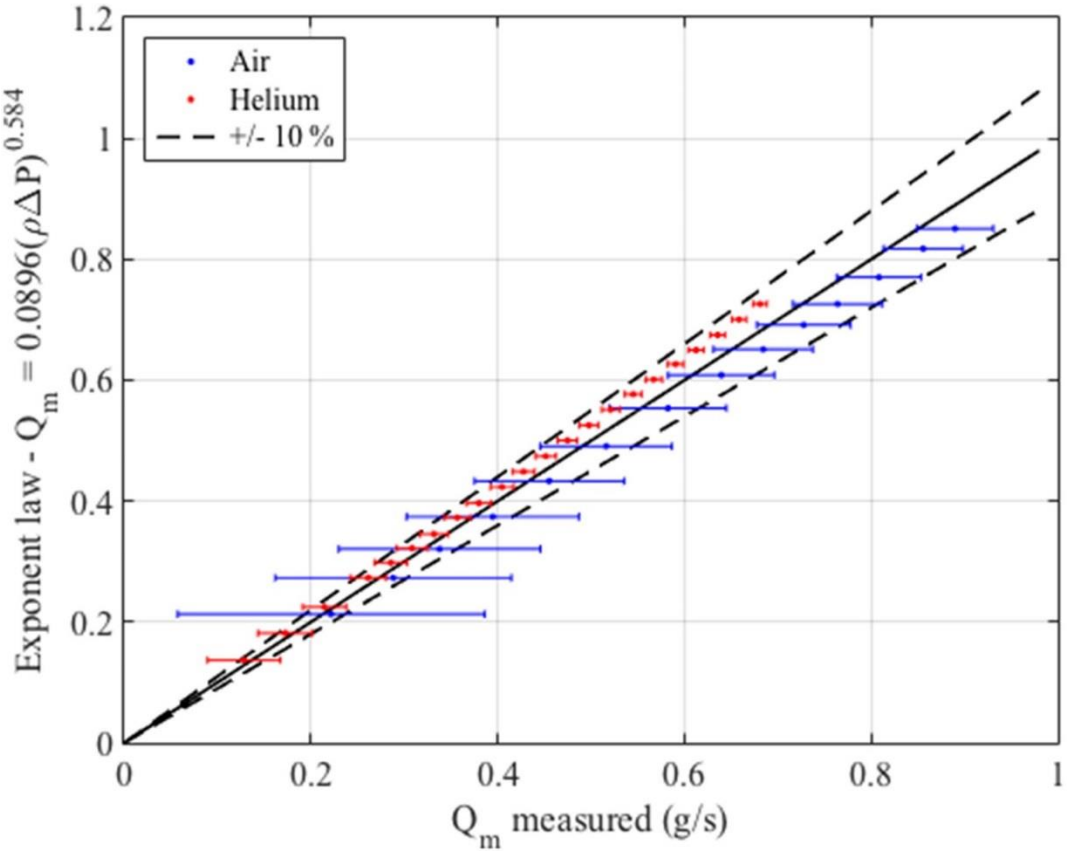

The HEPA filters were chosen to obtain an airflow resistance similar to the theoretical reduced-scale values needed to ensure a similarity of filter head losses.

Ventilated ducts consisting of standard PVC ducts were dimensioned based on the constraints exposed by Le Roux (Le Roux et al., 2012).

The heat release scenario was reproduced inside the reduced-scale model by a helium injection. Helium flow rate can be determined to reproduce a heat source value (Lucchesi et al., 2011) by the following equation:

$$q_{inj} = \frac{\dot{E}_s}{c_p T_{amb} \left(Y_{He}\right)_{inj} \left(\rho_{amb} - \rho_{He}\right)} \quad (2)$$

The injection was performed with pure helium in order to limit mass injection impact on the model.

For the characterization steps and the wind tunnel tests, the models were equipped with 126 pressure taps where the pressure was recorded by PSI sensors at 200 Hz. The pressure was measured at each internal node (rooms and junctions between the ducts) and each boundary condition node (external

pressure measured at the ventilation system inlet, the exhaust chimney outlet and the outside of each external leak). For each measurement, several pressure taps were used to ensure homogeneity or the absence of defects within the taps. Two pressure taps were also located on each side of the orifice plates to determine the flow rates inside the ducts. These pressure measurements were associated with the helium concentration measurements in order to determine the mass leakage and ventilated flow rates. Helium concentration was measured inside the rooms. Leakage flow rate was measured using the calibrated laws of each perforated plate.

In order to determine the component air flow rates, these measurements were associated with the gaseous mixing density in the junctions. This density was deduced from the helium concentration using the following relation:

$$\rho = \rho_{He}\chi_{He} + \rho_{amb}\chi_{air} = \rho_{He}\chi_{He} + \rho_{amb}\left(1 - \chi_{He}\right) \quad (3)$$

From this relation, an equivalent temperature has been deduced:

$$T = \frac{\rho_{ref}T_{ref}}{\rho} \quad (4)$$

It should be noticed that relation (4) is based on the assumption of ideal gas.

The helium volumetric concentration measurements were performed with a portable sniffing leak detector (Alcatel ASM 100 HDS), which can be used to measure a wide range of helium concentrations.

4. Results and discussion

4.1. Wind tunnel experimental results

Experiments were carried out in the Jules Verne climatic wind tunnel of the CSTB. The external building architecture and the location of the external and internal air paths are presented in Figure 4.

Figure 4. External building architecture of the studied configuration, location of the external (coloured filled arrows) and internal (coloured dotted arrows) air paths and wind incidence angles.

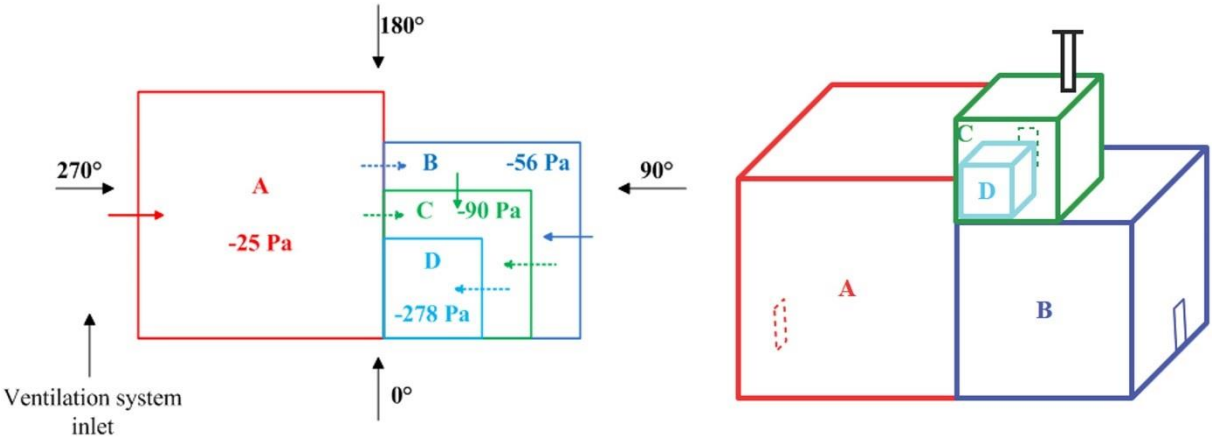

The pressure values given in Figure 4 are those measured for the reference case or design point. They were obtained with the operating point of the fans (Table 3) and no wind.

In addition, the black filled arrows have been included in Figure 4 with the aim of indicating the wind incidence angles tested afterwards (Table 4).

Table 4. Tests carried out in the Jules Verne climatic wind tunnel with the ventilation system on (•) or off (⊗).

	U_{wind} = 16 m s^{-1}				U_{wind} = 32 m s^{-1}				U_{wind} = 47 m s^{-1}	
θ $\dot{E}_s$	0°	90°	180°	270°	0°	90°	180°	270°	0°	180°
70 kW in Room A	•	•	•	•	•	•	•	•	•	–
	⊗	⊗	⊗	–	⊗	⊗	⊗	⊗	⊗	⊗
175 kW in Room A	–	–	–	–	•	–	•	–	–	–
0 kW Isothermal	•	•	•	•	•	•	•	•	•	•
	⊗	⊗	⊗	⊗	⊗	⊗	⊗	⊗	⊗	⊗

The configuration was studied in steady state at several wind incidences and velocities. The wind velocity was recorded with a Pitot tube placed 50 cm from the ceiling of the wind tunnel. The configuration was tested with the mechanical ventilation on, off and in protect mode (e.g., only the exhaust fan of rooms C and D in operation). Table 4 sums up the tests carried out. From each test, the mean nodal pressure values were determined.

The experimental results are presented here only for the thermal source located inside room A with the ventilation system on and off.

Contrary to an isothermal situation, a heat source inside the configuration requires taking into account a hydrostatic term which represents the weight of the air column between the ground and the altitude of the leak. The pressure difference between rooms decreases when the upstream temperature of the leak is lower than the downstream temperature. In this case, the density deviation $\Delta\rho$

is positive and the leakage air flow rate decreases. If the hydrostatic term is higher than the thermodynamic pressure difference $\Delta P(h=0)$,

then there is an air flow rate reversal.

4.1.1. Results with the ventilation system on

Pressure differences at leakages are caused by the ventilation system, the wind and the heat source. An analysis of the driving forces was carried out taking into consideration:

- the reference operating ventilation system effect, e.g. for a configuration without wind and heat release;
- the wind effect which is obtained with the ventilation system off and without heat release, named “Wind” in the figures;
- the isothermal case – “Isothermal” in the figures – which represents the wind effect which is obtained with the ventilation system on and without heat release;
- the full coupling – “Total” in the figures - is characterized by the pressure difference caused by the combined effects of the wind and the heat with the ventilation system on. This pressure difference was used to evaluate the natural driving forces compared to forces resulting from the ventilation system.

The pressure difference values at the bounds of the leakages are presented in Figure 5 for a wind velocity of 16 m s^{-1} and a 70 kW heat source in room A with the ventilation system on. The pressure differences are positive when the airflow direction is the same as the reference direction. For example, a positive pressure difference for a leakage between rooms A and C (A-C) means that the airflow direction is from room A to room C. For the external leaks, a positive pressure difference for a leakage between the exterior and the room A (Out. – Room A) means the airflow direction is from the outside to the room A.

Figure 5. Pressure difference values at the bounds of the leaks with a 70 kW heat source in room A, with the ventilation system on and a wind velocity of 16 m/s.

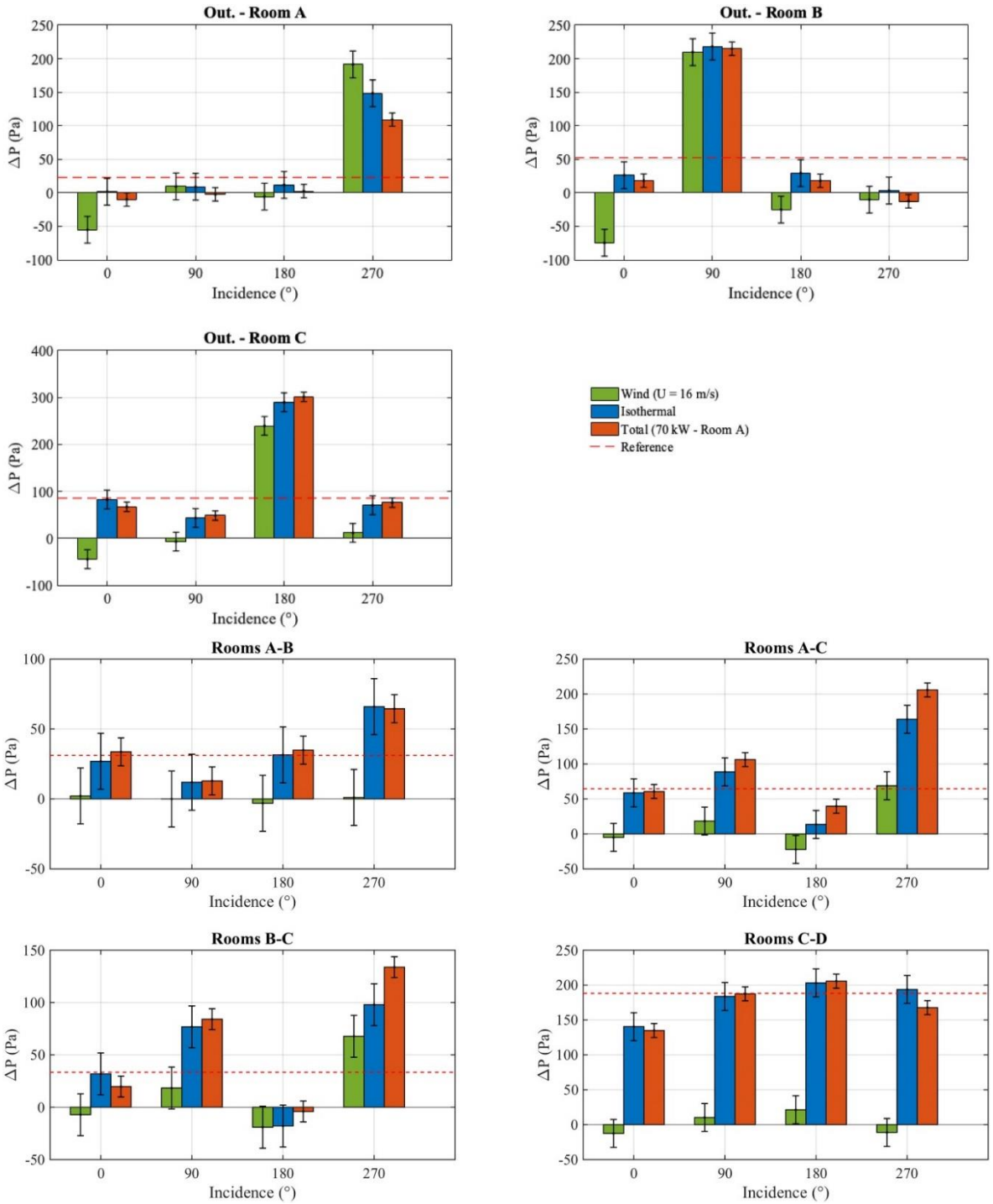

The air flow rate reversals are change in flow direction and obviously in the sign of the pressure difference. They may be caused by the thermal effects. For the results shown in Figure 5 and compared to the isothermal case, they are identified especially at the external leakage of room A for wind incidences of 0° and 90° and at the external leakage of room B for a wind incidence of 270°. The pressure difference at the bounds of these leaks caused by the wind and the ventilation system are much lower than the reference configuration. For a wind incidence of 0°, the wind creates a depression on the external leakage of room A. The pressure difference between the outside and the inside of room A becomes lower than the reference case. The heat source generates a decrease of the depression inside room A. The pressure difference between the outside and the inside of room A becomes negative and the flow is directed to the outside.

For internal leakages, the ventilation system determines the overall pressure difference, except for the leak linking rooms B and C for a wind incidence of 180°, because this is the incidence where the external leakage of room C is upwind.

Finally, the hydrostatic term resulting from the heat source is globally very low compared to the pressure cascade produced by the ventilation system.

The effects of the heat source on indoor equivalent temperatures are presented in Figure 6. The increase in equivalent temperature caused by the heat released is quite low, except in room A.

Figure 6. Indoor temperature increase due to 70 kW and 175 kW heat sources in room A and with the ventilation system on.

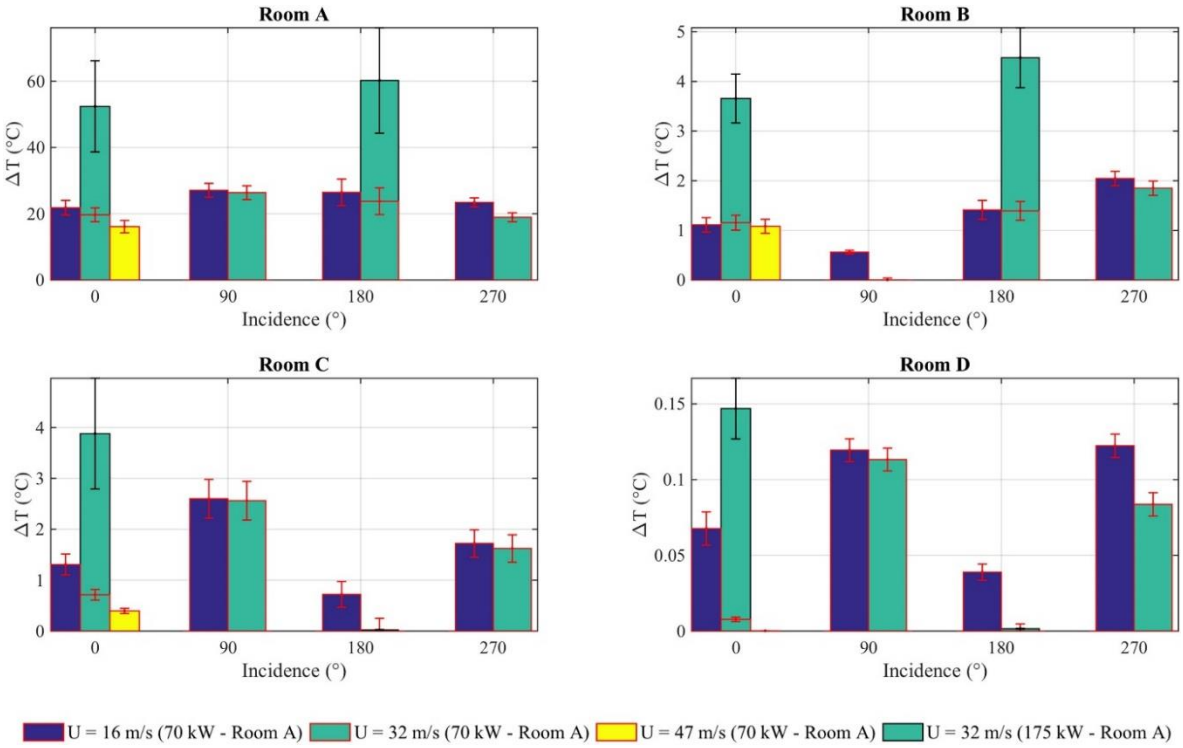

The wind had a low impact on the indoor temperature of room A. Indeed, for a wind incidence of 0°, the temperature increase varied from 16 °C to 27 °C for wind velocities ranging from 16 m s^{-1} to 47 m s^{-1}, respectively. The air renewal rate caused by the ventilation system is thus sufficiently important to limit the impact of the wind on the configuration.

For a wind incidence of 0°, an increase in the heat power resulted in a temperature rise of about 35 °C inside room A and 3 °C within room B and room C. The temperature difference inside room D is negligible.

The analysis of indoor temperature variations can provide information on air flow reversals. For instance, air flow rate reversals can be identified by the absence of temperature variation inside rooms B, C and D. For example, the air flow rate reversal between rooms A and B is highlighted by an absence of temperature variation inside room B for a wind incidence of 90° and a wind velocity of 32 m.s^{-1}.

Finally, a flow rate reversal between rooms C and D for a wind velocity of 47 m s^{-1} with a wind incidence of 0° is highlighted by the absence of an equivalent temperature increase inside room D.

4.1.2. Results with the ventilation system off

The impact of wind and heat was studied with the ventilation system off and for wind and heat release conditions similar to the cases studied with the ventilation system on.

The pressure differences at the bounds of the leaks were produced by the wind and the heat source. An analysis of the driving forces was carried out by taking into consideration:

- the wind effect which was obtained with the ventilation system off and without a heat source – "Wind" in the figures;
- the full coupling – "Total" in the figures - is characterized by the pressure difference produced by the combined effects of the wind and the heat.

The pressure difference values at the bounds of the leaks are presented in Figure 7 for a wind velocity of 16 m s^{-1} and a 70 kW heat source in room A.

Figure 7. Pressure difference values at the bounds of the leaks for a 70 kW heat source in room A and with the ventilation system off.

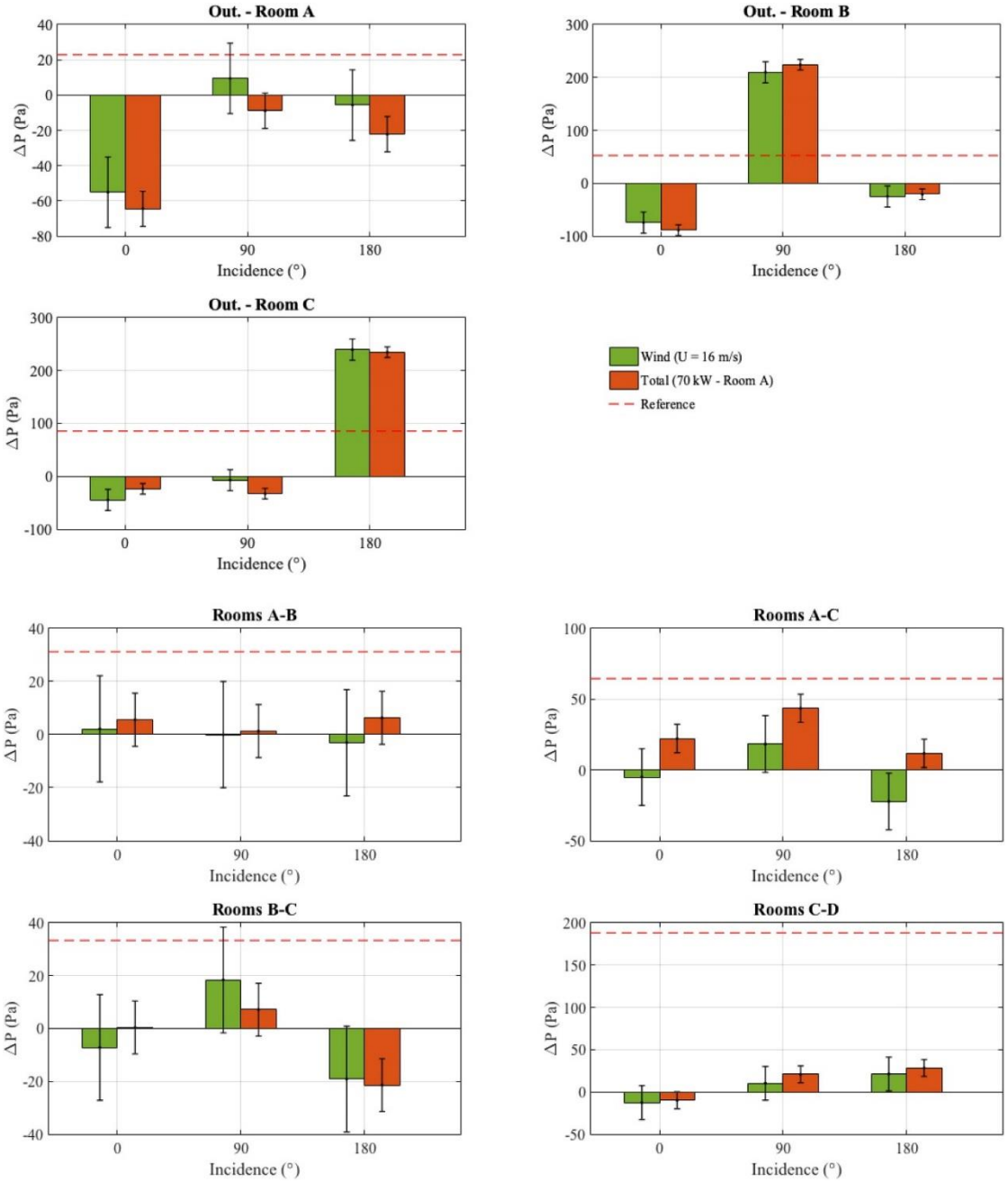

Even if the ventilation system is switched off, overall the heat released inside room A has a limited impact compared to the wind. The heat source effect is greater on the leakages from room A. Thus, it

is observed that for the external leakage to room A, heat accentuates the air flow rate reversal for wind incidences of 0° and 180°. The pressure differences at the bounds of this leak are 1.4 and 5.5 times higher, respectively, than in the isothermal situation.

Regarding internal leakages, the wind effect is lower than for external leakages. In fact, the pressure differences are systematically smaller than those obtained with the ventilation system at its reference operating regime. Heat coupled with a wind incidence of 90° causes a significant depression inside room B, resulting in a pressure difference at the bounds of the internal leakage between rooms B and C that is 3.6 times lower than the isothermal case without reversal. For a wind incidence of 180°, the heat produced an overpressure inside room A which modifies the air flow path of the internal leakage between rooms A and C.

The effect of heat on the indoor temperature as a function of wind incidence is presented in Figure 8.

Figure 8. Indoor temperature increase due to a 70 kW heat source in room A and with the ventilation system off.

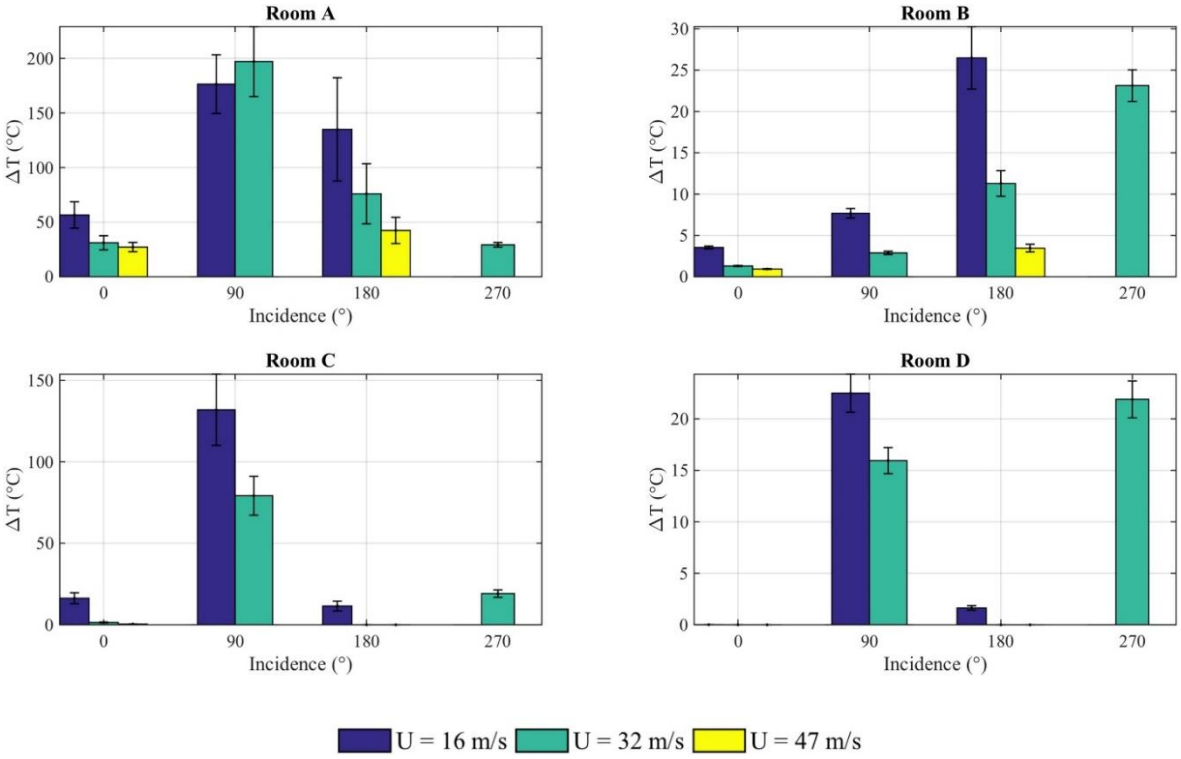

The temperature increase in room A is around 200 °C for a wind incidence of 90° (wind velocity of 16 m s^{-1}). The thermal source generates a negative pressure difference of −20 Pa at room A external leakage, which results in an air flow rate reversal for this leak.

For a wind incidence of 0°, the 42 °C temperature difference between rooms A and C results in a change of the airflow path between these two rooms compared to the isothermal configuration.

In addition, an air flow reversal is observed between rooms A and B for a wind incidence of 90° and a wind velocity of 32 m s^{-1}. This reversal causes a temperature increase inside room A. So, the temperature rise in room B is weak whereas high temperatures are observed inside room C. This temperature increase is caused by the leakage between rooms A and C.

Lastly, the indoor temperature of room D is always lower than the temperature inside room C because the room is only linked with room C.

To conclude, an analysis of the experimental results showed the importance of taking into consideration the effects of heat, in particular when the ventilation system is switched off. When the ventilation system is on, only wind effects may challenge the containment of the nuclear facility.

4.2. Comparison between numerical and experimental results

Numerical simulations were conducted with SYLVIA. To this end, the air flow resistance values obtained experimentally and calculated from the calibrated laws of the leaks, HEPA filters and ventilated ducts were used as input data in SYLVIA. Numerical and experimental configurations of the reference situation were compared. Then, the influence of wind was considered for these reference configurations using the mean external pressure values as the boundary conditions for each external path (ventilation system inlet, exhaust chimney and external leaks). Finally, a thermal source was introduced by means of a helium injection.

For each simulation, node pressures (23 values for each test), leakage air flow rates (7 values) and the indoor temperature of each room (4 values) were computed with SYLVIA and compared to the measured values.

The results were analysed using a "Bland-Altman" graph (Bland and Altman (1999)). This graphical presentation shows the absolute difference between the numerical and experimental values as a function of their mean values. We used Bland-Altman plots in order to investigate any possible relationship of the discrepancies between the experimental values and the simulated values. Moreover, an arbitrary interval of ±20% was considered on the plots for the relative differences. Even the value of the relative difference has been set to 20% arbitrarily, it should be noticed that it is the value of the Normalized Mean Bias Error (NMBE) recommended by the International Performance Measurement and Verification Protocol (IPMVP, 2012) for model calibration purposes.

4.2.1. Comparison with the ventilation system on

Figure 9 shows the indoor pressure differences between the experimental and the numerical values obtained for the configuration with the ventilation system on and 70 kW of heat released into room A. The values are given for all the nodes of the ventilation network (results for the rooms are highlighted) as a function of wind incidence and for three wind velocities, i.e., 16 m s^{-1}, 32 m s^{-1} and 47 m s^{-1}, respectively.

Figure 9. Indoor pressure difference between the experimental and numerical values (ventilation system on and 70 kW of heat released into room A).

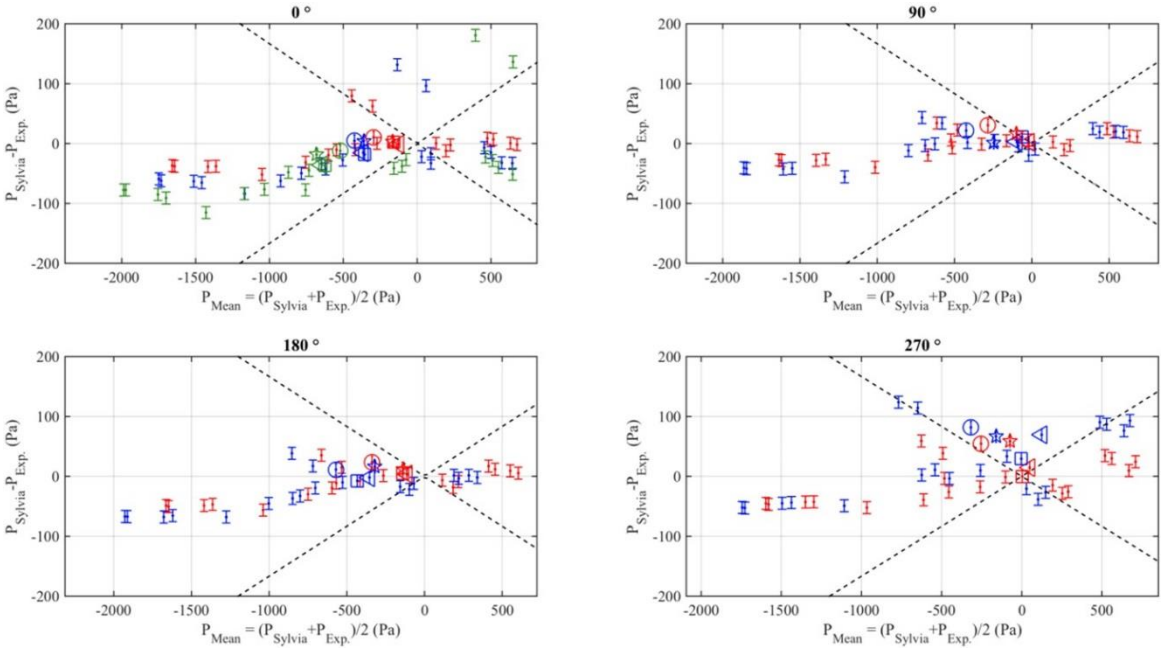

The experimental pressures are quite well reproduced by SYLVIA for the 90° and 180° wind incidences since 95% of the pressure values have a relative difference that is lower than 20%. Higher values are observed for wind incidences equal to 0° and 270°, with 15% of the relative differences higher than

20%. Generally speaking, the pressure values are underestimated by SYLVIA for wind incidences of 0°, 90° and 180°, but are overestimated for the 270° wind incidence. The biggest differences are observed at the ventilation system inlet for wind incidences of 0° and 270°. For the wind incidence of 0°, the two values which have the most important discrepancies are located at the supply ventilation system upstream from the supply fan. The pressure tap which was used as boundary condition of the supply ventilation system on SYLVIA would to be located in an unsteady zone of the flow.

From Figure 10, it can be observed that the experimental and numerical values are generally quite similar. The relative differences are less than 20% for 76% of the values. The largest differences are observed for the external leakages where there is a direct interaction with the external environment. Some of the differences can be explained in two ways. First, in some conditions, the pressure losses are lower than the measurement uncertainties. Second, wind turbulence can produce an unsteady leakage air flow rate. So, for very low mean values, the instantaneous air flow rate fluctuates between positive and negative values, resulting in a very low accuracy for the mean measured values. This phenomenon was observed and analysed by Le Roux (Le Roux (2011)).

Figure 10. Leakage air flow rate difference between the experimental and numerical values (ventilation system on and 70 kW of heat released into room A).

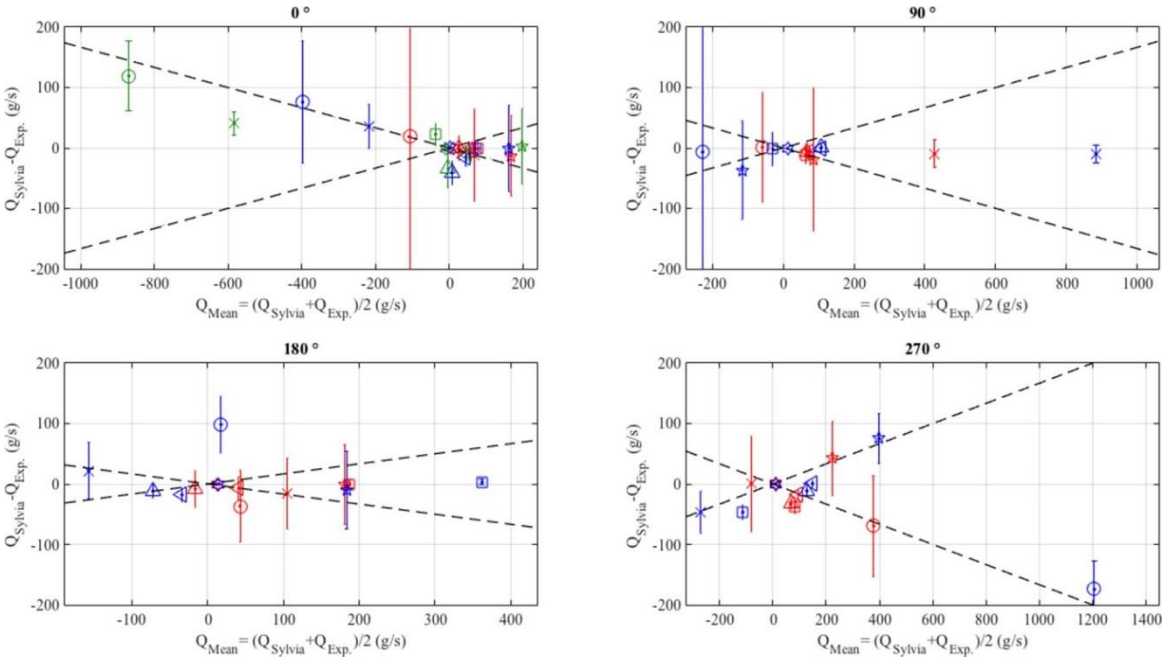

Figure 11 shows the differences between the experimental and numerical values of the indoor temperatures for the rooms.

Figure 11. Indoor temperature difference between the experimental and numerical values (ventilation system on and 70 kW of heat released into room A).

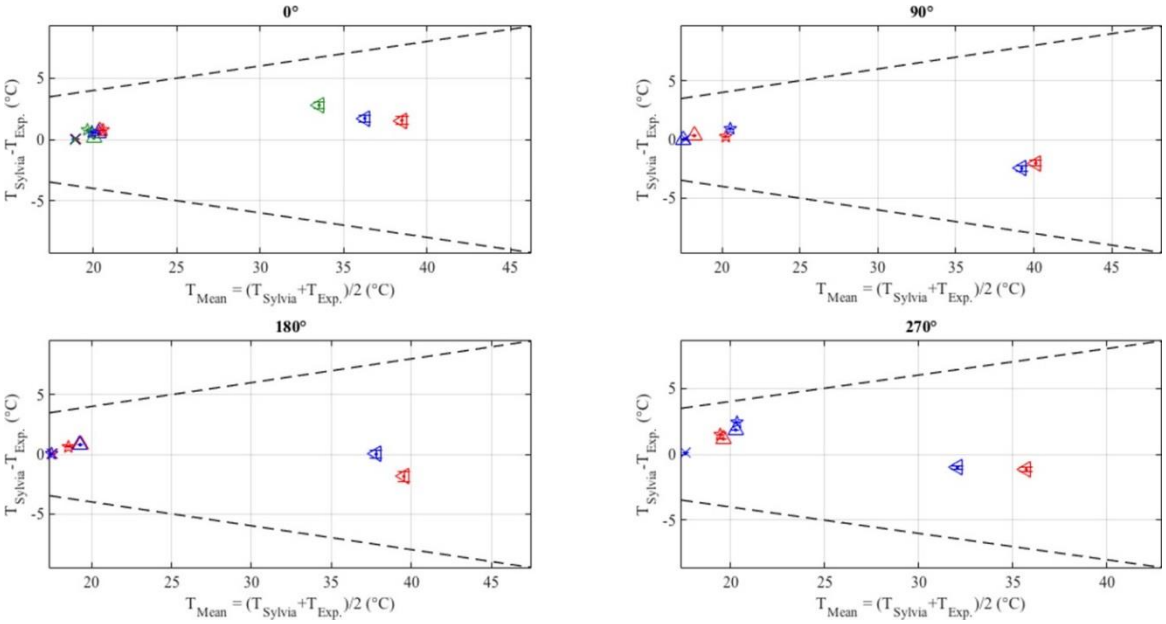

It can be observed that the experimental and calculated indoor temperature values are very close. In addition, the temperature of room A is very well reproduced by SYLVIA regardless of the wind conditions. Thus, the absolute difference is lower than 2.8 °C i.e., a relative difference of 8.3%.

4.2.2. Comparison with the ventilation system off

Figure 12 shows the indoor pressure differences between the experimental and numerical values obtained for the configuration with the mechanical ventilation off and for 70 kW of heat released into room A. The values are given as a function of wind incidence and for three wind velocities namely 16 m s^{-1}, 32 m s^{-1} and 47 m s^{-1}, respectively.

Figure 12. Indoor pressure difference between the experimental and numerical values (ventilation system off and 70 kW of heat released into room A).

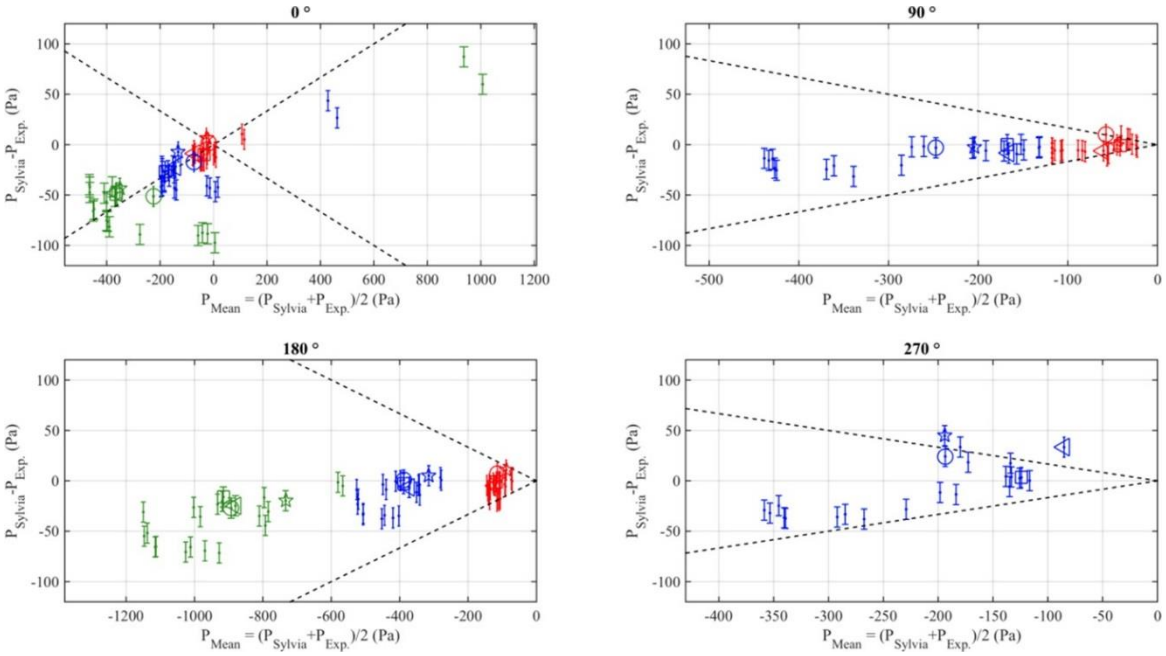

The indoor pressures calculated with SYLVIA are quite close to those measured for wind incidences of 90°, 180° and 270° since the relative differences are lower than 20% for about 95% of the values. Important disparities between measured and calculated pressures are observed for a wind incidence of 0°.

Figure 13 shows the leakage air flow rate differences between the experimental and numerical values computed for the ventilation system off and for 70 kW of heat released into room A.

Figure 13. Leakage air flow rate difference between the experimental and numerical values (ventilation system off and 70 kW heat released into room A).

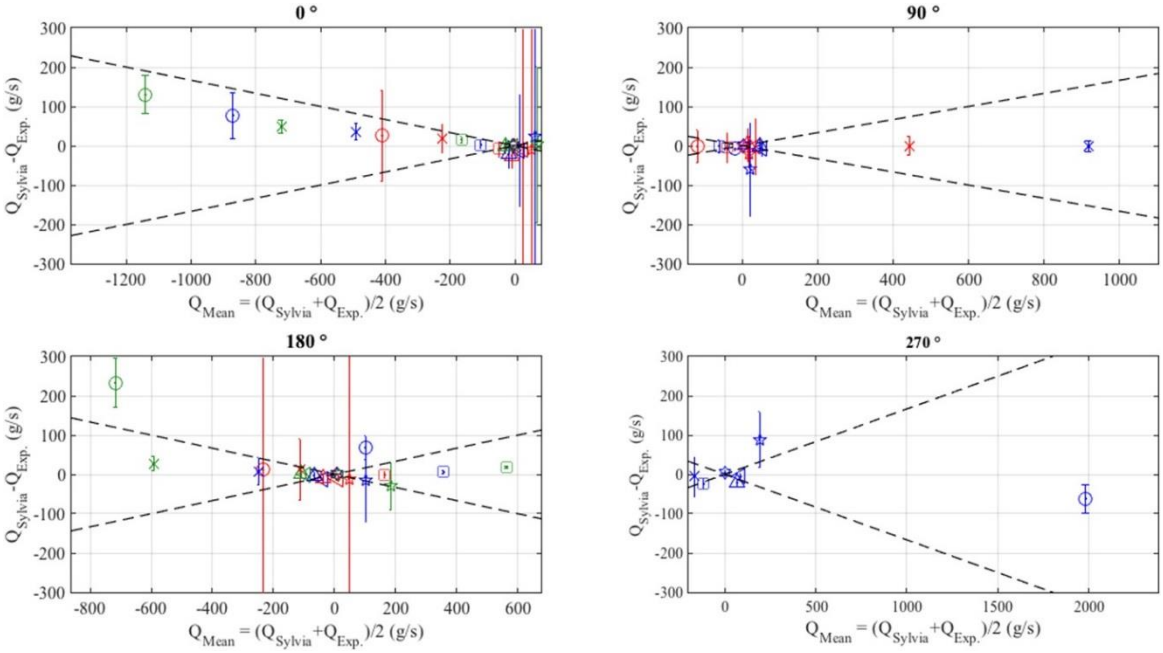

In general, when the ventilation system is turned off, the leakage air flow rates calculated with SYLVIA are very close to the measured rates since the relative differences are lower than 20% for around 67% of the values, regardless of the wind incidence and velocity. Thus, the results are quite similar to those obtained with the ventilation system on.

Figure 14 compares the experimental and numerical values of the indoor temperatures.

Figure 14. Indoor temperature difference between the experimental and numerical values (ventilation system off and 70 kW of heat released into room A).

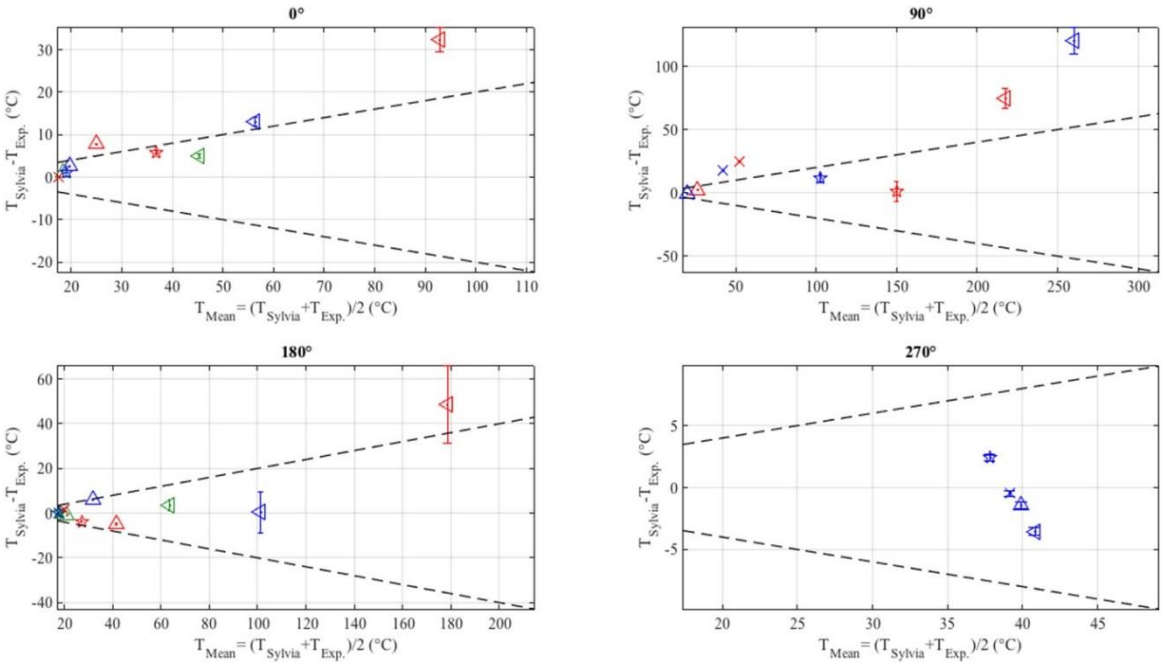

In general, the indoor temperatures computed with SYLVIA are overestimated. The relative difference could be higher than 46% and increases with wind velocity for a wind incidence of 180°. There are many explanations for these differences and additional studies are necessary in order to explain them accurately. The biggest differences were identified inside room A. The equivalent temperature was assumed to be homogeneous in the room. This hypothesis was no longer valid when the ventilation was switched off. Additional measurement points of the helium concentration would be required in order to have a most accurate mean equivalent temperature inside the room. Moreover, in this configuration, the flow inside the configuration is more sensitive to fluctuations induced by the wind tunnel.

4.2.3. Specific study of leakage air flow rate reversal

The analysis of the experimental results carried out highlighted the leakage air flow rate reversals caused either by the wind or by the heat released into a room. The objective here was to evaluate the capacity of SYLVIA to predict air flow rate reversals. To this end, we first selected the main air flow reversals we had observed in the experiments.

Then, we compared the numerical and experimental leakage air flow rates obtained under isothermal conditions and the experimental and numerical reverse leakage air flow rates resulting from 70 kW of heat released into room A under the same conditions (Figure 15).

Figure 15. Numerical and experimental leakage air flow rates under isothermal conditions (purple and blue bars) and reverse leakage air flow rates resulting from 70 kW of heat released into room A (green and yellow bars).

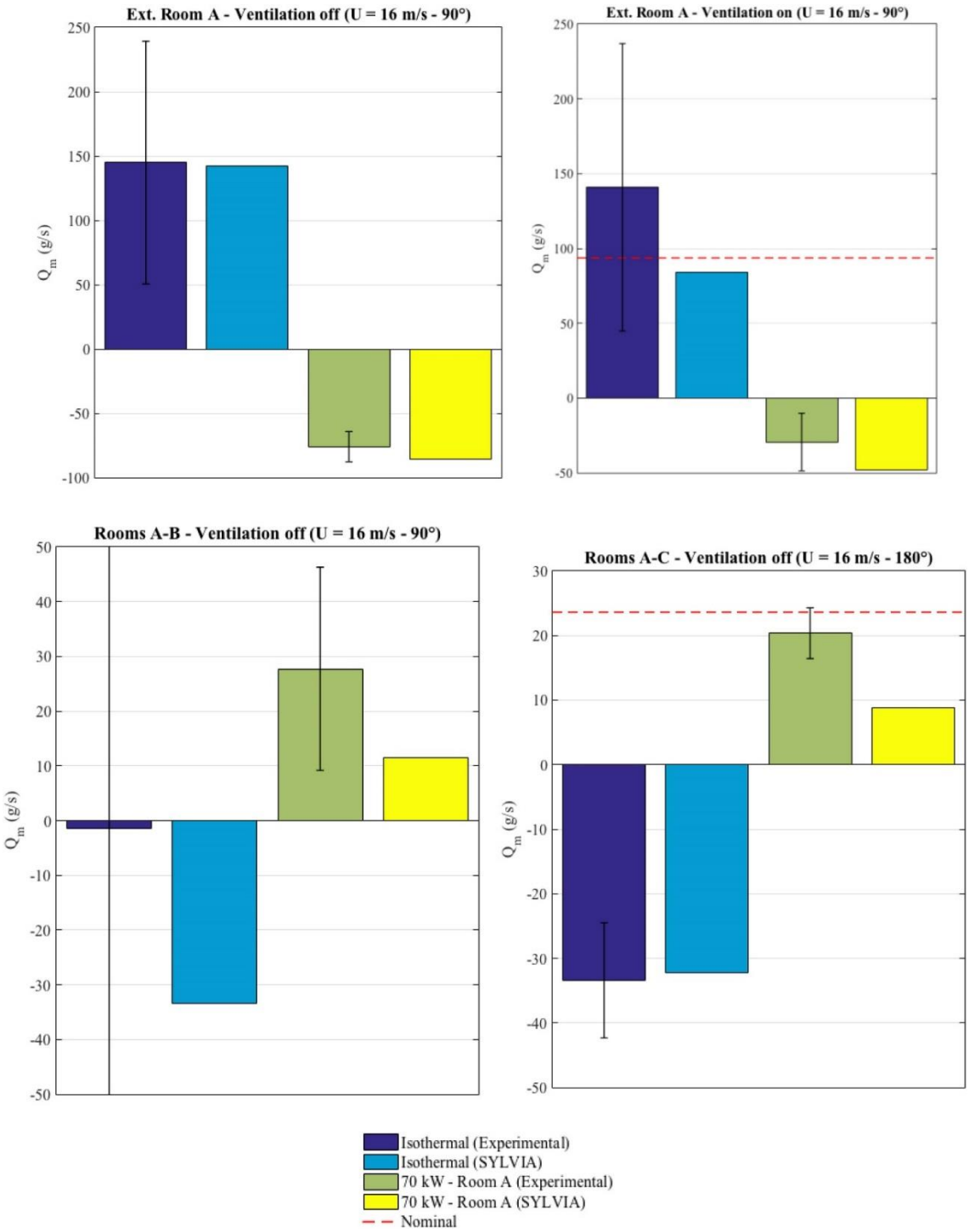

The leakage air flow rate reversals caused by heat released into room A are observed at the external and internal (rooms A and B, and rooms A and C) leakages of room A. When the ventilation is switched on, the air flow rate reversals caused by the heat source are located only at the external leakage of room A, where the heat source is located. In this case, the pressure differences between the rooms, which are provided by the ventilation system, are too large to cause an air flow rate reversal.

In general, the differences between the measured and calculated flow rates are included in the measurement uncertainty interval. The most important differences are located at the internal leakage linking rooms A and B because of low pressure differences between the rooms. In the case of the internal leakage between rooms A and C with a wind incidence of 180° and the ventilation off, the differences between the measured and calculated flow rate is higher than the measurement uncertainty. These large disparities occur for low flow rates. However, for each case, SYLVIA was able

to predict the leakage air flow rate reversals, proving the capacity of this numerical code to simulate accurately the loss of containment in nuclear facilities.

5. Conclusions and perspectives

The influence of wind on airflows inside mechanically ventilated nuclear facilities was studied for non-isothermal cases. To this end, a new methodology was developed to study non-isothermal flows in the steady state inside nuclear facilities equipped with ventilation systems. This methodology was then applied to a reference configuration representing a nuclear facility, for which the influence of wind was studied in a wind tunnel and the buoyancy effect was analysed using a helium injection system.

Leakage air flow rate reversals were identified that varied with external overpressures and depressions generated by wind. These reversals of air flow rates led to a partial or total loss of pollutant containment inside the nuclear facility.

Heat released inside a building results in density and pressure variations. This study of the pressure differences at the bounds of leakages induced by wind, heat and the ventilation system highlighted the low impact of heat, in the range of thermal power studied, when the ventilation system is on. Thus, it was observed that only wind can generate a variation in pressure that is sufficiently high to result in a loss of confinement.

Conversely, the temperatures inside the rooms increased significantly when the ventilation system was switched off, especially in the room where heat was released. The result was an increase in the pressure difference at the bounds of the leaks, including the external leaks. In addition, under some conditions, reversals of leakage air flows were observed with a loss of containment in the nuclear facility.

In this study, the numerical results given by SYLVIA were compared to the experimental data obtained using a wind tunnel.

Though some differences between the measured and computed results were underlined in specific cases, mostly because of experimental uncertainties, notably with the ventilation system off, the results were in good agreement. Furthermore, SYLVIA showed a good capacity to predict leakage air flow rate reversals due notably to heat release in a room and with the ventilation system off.

An important aspect that should be considered in the future is an extension to a two-zone model. Indeed, the approach used for the current study was limited to indoor ambients that are considered to be homogeneous in terms of pressure and temperature. Studies on two zones could provide a better simulation of thermal indoor stratification and pollutant concentration distribution.

Disclosure statement

No potential conflict of interest was reported by the authors.

Notes on contributors

Thomas Le Dez is engineer in Inovertis group, society specialized in innovative process. His work focuses on the improvement and maintenance of ventilation systems, mainly in the nuclear facilities. The software SYLVIA is used in order to design the ventilation systems of several facilities.

Jérôme Richard is a Dr. engineer at the French Institut de Radioprotection et de Sûreté Nucléaire (IRSN). He is the head of the Laboratory of Experiments and Modelling in Airborne dispersion and Containment. His work focuses on the modelling of thermal airflows and pollutants transfers inside the nuclear facilities, especially in ventilation networks.

Christian Inard is Professor at La Rochelle University, Department of Civil Engineering. His research activities are focused on design of low energy buildings, indoor thermal comfort and indoor air quality, HVAC systems modelling and control, and urban microclimate modelling and experiment.

Nicolas Le Roux is a Dr. engineer at the French Institut de Radioprotection et de Sûreté Nucléaire (IRSN), in the Laboratory of Experiments and Modelling in Airborne dispersion and Containment. His work focuses on the numerical and experimental characterization of airflows inside the nuclear facilities, in particular in ventilation networks. He conducted a PhD thesis on the reduced-scale study of airflows inside mechanically ventilated buildings subjected to wind.

François Demouge is a Research Engineer at the CSTB (Scientific and Technical Center for Building). He is part of the Numerical Modelling Group of the Climatology, Aerodynamics, Pollution and Epuration Department. His work focuses on the performance assessment of Ventilation Systems with regards to Indoor Air Quality, Thermal comfort and Energy Savings.

Xavier Faure is a Research Engineer at the CSTB (Scientific and Technical Center for Building). His work mainly focuses on thermo-aeraulic fields and he is head of the ventilation laboratory for standard evaluation of ventilation devices.

Laurent Ricciardi is an engineer at the French Institut de Radioprotection et de Sûreté Nucléaire (IRSN). He is the deputy head of the Airborne pollutants and Containment Department. His work focuses on modelling of airflows and gaseous/particulate pollutants transfers inside the nuclear facilities, in normal, degraded or accident situation.

Nomenclature	
c_p	Heat capacity at constant pressure ($J.kg^{-1}.K^{-1}$)
$\dot{E}_s$	Thermal power (W)
h	Height (m)
$\dot{m}_f$	Mass flow rate ($kg.s^{-1}$)
P	Pressure (Pa)
Q	Volumetric flow rate ($m^3.s^{-1}$)
R	Air flow resistance ($kg^{2-n}.m^{-4}.s^{n-2}$)
S	Area (m^2)
T	Temperature (K)
U	Wind velocity ($m.s^{-1}$)
Y	Mass fraction (-)
z	Altitude (m)

Greek Symbols	
θ	Wind incidence (°)
ρ	Density ($kg.m^{-3}$)
χ	Volumetric fraction (-)
ΔP	Pressure difference (Pa)
ΔT	Temperature difference (°C)

Exponent	
n	Exponent law

Subscripts	
amb	Ambient
Exp.	Experimental data
He	Helium
Mean	Mean values
n	Node
ref	Reference
Sylvia	SYLVIA data

References

- Bland, J. M., & Altman, D. G. (1999). Measuring agreement in method comparison studies. *Statistical Methods in Medical Research*, *8*(2), 135–160. [Crossref], [Web of Science ®], [Google Scholar]
- Chen, H. X., Liu, N. A., & Chow, W. K. (2011). Wind tunnel tests on compartment fires with crossflow ventilation. *Journal of Wind Engineering and Industrial Aerodynamics*, *99*(10), 1025–1035. [Crossref], [Web of Science ®], [Google Scholar]
- Hunt, G. R., & Linden, P. F. (2001). Steady-state flows in an enclosure ventilated by buoyancy forces assisted by wind. *Journal of Fluid Mechanics*, *426*, 355–386. [Crossref], [Web of Science ®], [Google Scholar]
- Hunt, G. R., & Linden, P. F. (2005). Displacement and mixing ventilation driven by opposing wind and buoyancy. *Journal of Fluid Mechanics*, *527*, 27–55. [Crossref], [Web of Science ®], [Google Scholar]
- IPMVP. (2012). International Performance Measurement and Verification Protocol: Concepts and Options for Determining Energy and Water Savings, *Volume 1, Technical Report, Efficiency Valuation Organization*: *Washington, DC, USA*. [Google Scholar]
- International Organization for Standardization (ISO). (2004). Nuclear facilities. Criteria for the design and operation of ventilation systems for nuclear installation other than nuclear reactors. (ISO 17873: 2004). [Google Scholar]
- Le Dez, T. (2016). *Approche par similitude du couplage des effets thermiques et du vent sur les transferts de masse dans les réseaux aérauliques des bâtiments complexes* (Doctoral Dissertation). Retrieved from https://hal.archives-ouvertes.fr/tel-01661300. [Google Scholar]
- Le Roux, N. (2011). *Etude par similitude de l'influence du vent sur les transferts de masse dans les bâtiments complexes* (Doctoral Dissertation). Retrieved from https://hal.archives-ouvertes.fr/tel-00717838. [Google Scholar]
- Le Roux, N., Faure, X., Inard, C., Soares, S., & Ricciardi, L. (2012). Reduced-scale study of wind influence on mean airflows inside buildings equipped with ventilation systems. *Building and Environment*, *58*, 231–244. [Crossref], [Web of Science ®], [Google Scholar]
- Le Roux, N., Faure, X., Inard, C., Soares, S., & Ricciardi, L. (2013). Reduced-scale study of transient flows inside mechanically ventilated buildings subjected to wind and internal overpressure effects. *Building and Environment*, *62*, 18–32. [Crossref], [Web of Science ®], [Google Scholar]
- Li, Y., Delsante, A., Chen, Z. D., Sandberg, M., Andersen, A., Bjerre, M., & Heiselberg, P. (2001). Some examples of solution multiplicity in natural ventilation. *Building and Environment*, *36*(7), 851–858. [Crossref], [Web of Science ®], [Google Scholar]
- Lucchesi, C., Vauquelin, O., Pretrel, H., & Bournot, P. (2011). Doorway flow from a reduced scale isothermal air/helium approach. *International Journal of Thermal Sciences*, *50*(10), 1920–1929. [Crossref], [Web of Science ®], [Google Scholar]
- Prétrel, H., Le Saux, X., & Audouin, L. (2012). Pressure variations induced by a pool fire in a well-confined and force-ventilated compartment. *Fire Safety Journal*, *52*, 11–24. [Crossref], [Web of Science ®], [Google Scholar]
- Ricciardi, L., Gélain, T., & Soares, S. (2015). Experimental and numerical characterization of wind-induced pressure coefficients on nuclear buildings and chimney exhausts. *Nuclear Engineering and Design*, *292*, 248–260. [Crossref], [Web of Science ®], [Google Scholar]

- Vauquelin, O., & Megret, O. (2002). Smoke extraction experiments in case of fire in a tunnel. *Fire Safety Journal*, *37*(5), 525–533. [Crossref], [Web of Science ®], [Google Scholar]
- Vauquelin, O. (2008). Experimental simulations of fire-induced smoke control in tunnels using an "air-helium reduced scale model": Principle, limitations, results and future. *Tunnelling and Underground Space Technology*, *23*(2), 171–178. [Crossref], [Web of Science ®], [Google Scholar]
- Vaux, S., & Prétrel, H. (2013). Relative effects of inertia and buoyancy on smoke propagation in confined and forced ventilated enclosure fire scenarios. *Fire Safety Journal*, *62, Part B*, 206–220. [Crossref], [Web of Science ®], [Google Scholar]